Arabian Journal of Chemistry 16 (2023) 105318

Contents lists available at ScienceDirect

Arabian Journal of Chemistry

journal homepage: www.sciencedirect.com

Original article

Anticancer activity of zinc-nickel nanocomposite in lung cancer PC14 cells via modulation of apoptosis and P13K/mTOR pathway

Dawei Wang [a], Shuang Wu [a], Jian Fang [b,*]

[a] Department of Cardiothoracic surgery, Yantaishan Hospital, No.91 Jiefang Road, Zhifu District, Yantai, Shandong 264001, China
[b] Department of Thoracic Surgery, Yantai Yuhuangding Hospital, No. 20 Yuhuangding East Road, Zhifu District, Yantai, Shandong 264000, China

ARTICLE INFO

Article history:
Received 10 January 2023
Accepted 28 September 2023
Available online 4 October 2023

Keywords:
Cancer
Zinc-nickel nanomaterial
Apoptosis
P13K/mTOR pathway

ABSTRACT

Advanced innovations for combating variants of aggressive cancer and overcoming drug resistance are desired. In cancer treatment, nanoparticles (NPs) have the capacity to specifically and compellingly activate apoptosis of cancer cells. There is also a pressing need to develop innovative anti-cancer therapeutics, and recent research suggests that ZnO nanoparticles hold great potential. The current exploration was designed to fabricate the zinc-nickel nanomaterial (Zn-Ni NPs) and examine its *in vitro* anticancer effects on lung cancer cell. In ultraviolet–visible spectroscopy (UV–Vis), the bands at the wavelengths of 219, 265, 397, and 458 nm are related to the surface plasmon resonance of the synthetic Zn-Ni NPs. In fourier transform-infrared spectroscopy (FT-IR), the peaks of 449, 618, 659, 662, and 693 can be assigned to Zn-O or Ni-O bonds. The cytotoxicity of the Zn-Ni NPs (1 to 1000 μg/mL) were studied by the MTT assay and the IC50 dose for Zn-Ni NPs were found at 77 μg/mL. The different fluorescent staining assays such as Dichloro-dihydro-fluorescein diacetate, Rhodamine-123, and dual staining were performed to investigate the influence of Zn-Ni NPs on the apoptosis, matrix metalloproteinase status, and reactive oxygen species accumulation in the PC14 cells. The status of inflammatory markers such as IL-6, COX-2, TNF-α, and NF-κB in the PC14 cells were studied. The increased dosage of Zn-Ni NPs were effective repressed the growth of PC14 cells. The PC14 cells treated with Zn-Ni NPs revealed a significantly fewer proliferating cells and more apoptotic cells when compared with control. The Zn-Ni NPs also inhibited the phosphorylation of mTOR and Akt, reducing tumor volume and weight. PC14 cells phosphorylated mTOR, cyclin D1, Akt, and PI3K in response to Zn-Ni NPs. The findings were revealed that the fabricated Zn-Ni NPs considerably increased the ROS accumulation and apoptosis in the PC14 cells. Zn-Ni NPs also enhanced mitochondrial apoptosis through Bcl-2 protein-dependent signaling. In conclusion, Zn-Ni NPs might be promising candidate for lung cancer treatment.

1. Introduction

Cancer is the term designated to a group of diseases caused by uncontrolled cell growth and proliferation. There are various risk factors that contribute to the incidence of this pathology, and they are categorized into intrinsic and non-intrinsic. Intrinsic risk factors are related to spontaneous mutations that occur randomly in DNA replication, whereas non-intrinsic risk factors include events that can be either modifiable (e.g., smoking, alcohol consumption, nutrient intake, and exposure to chemical carcinogens) or endogenous (e.g., genetic susceptibility, errors in DNA repair machinery, and dysregulated hormone levels) (Bray et al., 2018; Liu et al., 2017). The distinct types of cancer are classified in accordance with their tissue or cell of origin and exhibit specific anatomic, histopathologic, molecular, genetic, and topographic features (Gospodarowicz et al., 2015; Cancer Today, 2022; Siegel et al., 2022). Lung cancer (LC) is the leading cause of cancer related deaths worldwide; it is estimated that 236,740 persons were diagnosed with lung cancer in 2022, whereas 130,180 will probably die because of this disease (Cancer of the Lung and Bronchus-Cancer Stat Facts, 2022). The treatment of lung cancer and its subtypes, small cell lung cancer (SCLC) and non-small cell lung cancer (NSCLC), is based on chemotherapy, radiotherapy, immunotherapy, and targeted therapy regimens. However, despite their possible efficacy, their administration entails serious adverse effects, limited specificity, drug resistance development, and the possibility

* Corresponding author.
E-mail address: FJ_xwk@hotmail.com (J. Fang).
Peer review under responsibility of King Saud University.

Production and hosting by Elsevier

https://doi.org/10.1016/j.arabjc.2023.105318
1878-5352/

of relapse. Thus, the consideration of new and safe therapeutic alternatives is needed.

Nanotechnology is a fast-evolving field focused on producing structures to overcome agricultural, industrial, and therapeutic challenges. Objects found at the nanometric scale (1–100 nm) are known as nanomaterials and are categorized into organic and inorganic. Organic NMs include liposomes, dendrimers, micelles, and biopolymeric nanoparticles (NPs). For biomedical purposes, organic nanomaterials are design for drug or nucleic acid delivery, bone regeneration, wound healing, and imaging applications (Khalid et al., 2020). However, for cancer treatment, their implementation is limited, due to their low encapsulation efficacy, low mechanical strength, instability, and restricted cellular internalization (Cheng et al., 2021; Virlan et al., 2016).

For the diagnosis and treatment of lung cancer, a variety of nanoparticle systems have been developed, including organic, inorganic, metallic, and polymeric nanoparticles (Mottaghitalab et al., 2019). Gholami et al. discussed the recent research and also various ongoing studies in the clinical application of dendrimers, liposomes, and polymeric micelle nanoparticles for the management of lung cancer (Gholami et al., 2023). Its interaction with the surface of the respiratory system plays a significant role in determining the toxicity of the nanoparticle. The potential toxicity of nanoparticles to the pulmonary surfactant, alveolar epithelium, and immune system should be considered in developing new nanoformulations for lung cancer treatment, and this has been discussed by researchers (Li et al., 2022).

In this research we focus on the green synthesis of zinc-nickel nanomaterial (Zn-Ni NPs) using *Curcuma longa* extract. Zn-Ni NPs were characterized using conventional techniques of spectroscopic, diffraction, and microscopic imaging to comprehend the structure, morphology, and size. Furthermore, the biological activity of Zn-Ni NPs including antioxidant, cytotoxicity, and anticancer activity were evaluated. The different fluorescent staining assays such as Dichloro-dihydro-fluorescein diacetate, Rhodamine-123, and dual staining were performed to investigate the influence of Zn-Ni NPs on the apoptosis, matrix metalloproteinase status, and reactive oxygen species accumulation in the lung cancer PC14 cells.

2. Material and methods

2.1. Chemicals

All materials were purchased from Sigma Aldrich, USA.

2.2. The preparation of zinc-nickel nanomaterial (Zn-Ni NPs)

First, 2 g of grinded *Curcuma longa* leaf was added to 100 mL of distillated water to boil for 15 min. The extract was filtered through a filter paper. To green synthesis of bi-metallic nanocomposite of Ni/Zn, 10 mL of flax extract was added to 20 mL of Ni $(NO_3)_2{\cdot}6H_2O$ and $Zn(NO_3)_2{\cdot}4H_2O$ in concentration of 0.1 M with 1:1 ratio. The pH was adjusted at 10 using NaOH 5%. The mixture was placed in an ultrasonic bath at 30 °C for 90 min. After 30 min. from the starting time, 1 mL of the chitosan solution (1% w/v in acetic acid 1%) was added drop-wise. The NPs was formed during reaction time with a creamy color. After the time, the residues were centrifuged at 10,000 RPM for 15 min. The formed nanocomposite was dried in an oven at 45 °C for 5 h. Zn-Ni NPs was kept in cold place before characterization.

2.3. The characterization of Zn-Ni NPs

UV–Vis. and FT-IR spectroscopy; XRD, SEM, and EDS techniques were used to characterize the biosynthesized Zn-Ni NPs. Different parameters of the nanoparticles, such as shape, particle size, fractal dimensions, crystallinity, and surface area are obtained by these techniques.

2.3.1. UV–vis spectrophotometry

The UV–Vis. spectra were obtained by a PhotonixAr 2015 UV–Vis. Spectrophotometer (200–800 nm).

2.3.2. FTIR analysis

The FT-IR spectra were recorded using a Shimadzu FT-IR 8400 in the range of 400–4000 cm^{-1}(KBr disc).

2.3.3. FE-SEM and EDX analyses

MIRA3TESCAN-XMU was used to report the FE-SEM images and EDS result.

2.3.4. X-ray diffractive analysis

The XRD pattern of Zn-Ni NPs was recorded in the 2θ range of 20–80° by a GNR EXPLORER instrument at a voltage of 40KV, a current of 30 mA, and Cu-Kα radiation (1.5406 Å).

2.4. MTT assay

In first, lung cancer PC14 placed in 1640-RPMI medium from GiBco manufacturer and was cultured after adding 10% bovine serum, 1% streptomycin and penicillin antibiotics and 2% glutamine. At this stage, the cell culture flasks were kept in an incubator with 5% CO_2 and 95% humidity at a temperature of 37 °C, and the culture medium was replaced every three days. In this step, flasks with 80% cell density were used (flasks filled with cells up to 80% of the bottom). First, the culture medium was removed from the surface of the cells and by adding 1 mL of trypsin for 3 min and then adding the same volume of medium to neutralize the effect of trypsin, all the cells were separated from the flask bottom. This cell suspension was centrifuged at 1200 rpm for 4 min. The liquid above the sediment was discarded and 1 mL of culture medium was added to the sediment. By taking 10 μl of the cell suspension and adding the same amount of trypan blue on the surface of the neobar slide, the number of living cells was counted. The number of 10,000 cells from this cell suspension was added to each well of 96-well plates and 180 μl of culture medium was added to it. In the next step, 20 μl different concentrations of nanoparticles were added to the wells. In this research, based on the conventional concentrations of nanoparticles at 0–1000 μg/ml, they were added to cells. Another group of cells was tested as a control, without adding nanoparticles and only by adding water instead of nanoparticles, and each experiment was done in four replicates. After 24, 48 and 72 h, the medium on the cells was replaced with a new medium. Then 20 μl MTT solution was added to each well and placed in a greenhouse for 4 h in the dark in a CO_2 incubator. During this time, the mitochondrial succinate dehydrogenase enzyme of living cells changes the yellow color of MTT solution to purple formazan crystals, which are insoluble in water. In the next step, 200 μl of DMSO (Dimethylsulfoxide) was added to the empty medium and shaken for 20 min to dissolve the light-producing crystals. In the last step, the absorbance was read with a wavelength of 492 and then 630 nm in an ELISA reader. Finally, the percentage of cell viability was calculated after dividing the optical absorbance by 100 (Han et al., 2020).

DCFH-DA staining technique was executed to investigate the ROS accumulation status in the PC14 cells. The MMP status in the NPs administered PC14 cells were examined by the Rhodamine 123 staining. The apoptotic incidences in the control and formulated NPs treated PC14 cells were studied by dual staining technique. Cell adhesion assays were used to evaluate the adhesive characteristics of control and formulated NPs treated PC14 cells.

Our real-time PCR technique measured the expression levels of NF-kβ, COX2, IL-6, TNF-α, Akt, mTOR P1K3, CyclinD1, Bcl-2, Caspase-3, and Bax (Han et al., 2020).

2.5. Statistical analysis

The collected data were analyzed by SPSS software and one-way analysis of variance and Duncan post hoc test. The one-way ANOVA and Tukey's test were executed. A p less than 0.05 were deliberated as significant.

3. Results and discussion

Recently, plants have been used for synthesizing metallic NPs due to their high therapeutic activities. The pollution created during the NPs biosynthesis by plant extract is almost zero. As a result, the herbal nanoparticles have very low environmental effects. But, the quantity and quality effects of metallic NPs depend on many factors such as the plant extract nature, extract concentration, temperature, metal salt concentration, pH, and reaction time (Han et al., 2020; Shaabani et al., 2008; Budarin et al., 2008; Dehnoee et al., 2023).

Nanotechnology is a branch of material science, recognized as one of the key technologies of the future. Nanomaterials are used in many different parts of human life and can provide solutions for technological and environmental challenges. These materials have unique properties due to their particle size used in several science fields such as medicine, engineering and technology (including electronics, environmental measurement, Raman spectroscopy of bacterial surface, antibacterial agent, drug delivery and water purification) (Elkhenany et al., 2020; Borm et al., 2006; Stapleton and Nurkiewicz, 2014; Patra et al., 2018). The application of nanomaterials in medicine, especially in drug delivery, has increased in the last decade. However, some nanomaterials have harmful effects, the most important of which is the poisoning of humans and animals (Itani and Al Faraj, 2019; Trojer et al., 2013; Liu et al., 2014; Zangeneh et al., 2020). For example, zinc oxide nanoparticles are liver function disorder and silver nanotoxicity in zebrafish embryos. In addition, this toxicity can directly harm human health, which hurts reproduction and fetal development. These factors have researched to develop non-toxic nanomaterial production methods (Han et al., 2020;Zangeneh et al., 2020). Therefore, to minimize waste products use and maximize the chemical processes efficiency, the basic principles of green chemistry should be adopted. Therefore, any chemical process or synthetic pathway must meet these principles with environmentally non-toxic chemicals and benign solvents (Han et al., 2020; Dehnoee et al., 2023).

In this study we have described an eco-friendly way for the fabrication of Zn-Ni NPs over an aqueous extract of *Curcuma longa* as stabilizing/reducing agent without using harmful toxic reagents. Thereafter, morphological structure and physicochemical characteristics of the NPs were ascertained by a range of analytical systems like UV–Vis, SEM, EDX, XRD, and FT-IR.

The synthesis of Zn-Ni NPs can be detected easily by visible observations, as shown in Fig. 1, where the color solution changed. In UV–Vis, the bands at the wavelengths of 219, 265, 397, and 458 nm are related to the surface plasmon resonance of the synthetic Zn-Ni NPs. In FT-IR, the peaks of 449, 618, 659, 662, and 693 can be assigned to Zn-O or Ni-O bonds. The appearance of other bands at various wavenumbers of 2920, 1388–1656, 1069, and 3436 cm^{-1} display the presence of C–H, C = C, C = O, C-O, and O–H bonds (Fig. 1).

Instead of the peaks at 8.14, 7.56, and 0.91 KeV for NiKβ, NiKα, and NiLα; and the signals at 9.61, 8.71, and 1.06KeV for ZnKβ, ZnKα, and ZnLα respectively are the major peaks for the metal elements in the synthesized bi-metallic NPs. Besides, the peaks at 0.51 KeV and 0.28 KeV can be assigned to oxygen and carbon (Fig. 2).

The peaks at different 2 theta values of 78.91, 75.10, 62.56, 56.41, 42.97, 37.08, 36.12, 34.20, and 31.81 are very close to those of NiO (standard database JCPDS card no. 1313–991) and ZnO (standard databaseJCDD PDF card no. 01–080-3002) with a little shift (Fig. 2).

The surface morphology, shape and size of the prepared Zn-Ni NPs were analyzed by FE-SEM image (Fig. 3). Apparently it depicts a layered sheet like structure where the globular particles are embedded. It seems being an agglomerated form which is made due to manual preparation of sample during SEM analysis. Mean diameter of the nanocomposite particles are within 20–70 nm. (See Fig. 4).

Today, the use of nanomaterials in combination with anticancer drugs is increasing widely, and the use of these compounds has many applications in medicine. One of the practical aspects of nanomaterials is to combine them with anticancer drugs so that the drug can be delivered to the cell with a higher effect, also, its toxicity on healthy cells can be decreased (Shaabani et al., 2008; Budarin et al., 2008; Dehnoee et al., 2023; Elkhenany et al., 2020). Due to the rising death prevalence caused by cancers and defects in chemotherapy and radiotherapy methods in cancer advanced stages, it needs to find modern techniques to control and cure cancer. Nanoparticles used with a diameter of 100 nm or less with anticancer supplements to target cancer cells in cancer projects are research first priority (Borm et al., 2006; Stapleton and Nurkiewicz, 2014; Patra et al., 2018; Itani and Al Faraj, 2019). A significant relationship between nanoparticle size and cytotoxic effects has been reported. One of the most common nanoparticles in this field is zinc nanoparticles, which are considered one the potential anticancer agents. Studies show that zinc nanoparticles cause the death of cancer cells by two mechanisms (Itani and Al Faraj, 2019; Trojer et al., 2013; Liu et al., 2014; Zangeneh et al., 2020). One is its direct effect or interaction with cell compounds (RNA, DNA and protein and cell structures (organelles and cell membranes), which leads to the induction of cell death. Second, their indirect effect creates toxic oxygen radicals, which ultimately promote cell death (Liu et al., 2014; Zangeneh et al., 2020; Ma et al., 2022; Lademann et al., 2007).

Based on the MTT test, the results of optical absorption (OD) in concentrations of 0–1000 μg/ml nanoparticles were compared to the cell survival rate after 24, 48 and 72 h. It is necessary to explain that the selected concentration range of nanoparticles was based on its anti-cancer effects in various articles and also the preliminary studies conducted in the laboratory. The graphs 4 and 5 show the survival percentage of cancer and normal cells after treatment with nanoparticles with different concentrations (0–1000 μg/ml). As you can see in this Fig. 5, the highest percentage of cancer cell survival was obtained at a dilation of 1000 μg/ml in 72 h. The graph show that IC_{50} = 77 μg/ml is a concentration of nanoparticles in which 50% of the PC14 lung carcinoma cells in the culture medium are destroyed. The results show that after 72 h, the survival rate of cancer cells in different concentrations decreased as the nanoparticles concentration raised, until no viable cells were seen at the dilation of 1000 μg/ml. The best cytotoxicity was seen at a dilation of 1000 μg/ml. The results show that within three days, the survival percentage of cancer cells in different concentrations decreased as much as the concentration of nanoparticles increased. Also, the statistical analysis related to the results of all data shows less than 0.05, which is considered a significant level. In other words, nanoparticles cause cytotoxicity or anticancer effect in cancer cells, which has the lowest percentage of cell survival in 72 h with a concentration of 1000 μg/ml.

Fig. 6 reveals the gene expression of NF-κB, IL-6, COX-2, and TNF-α are seen after Zn-Ni NPs are treated for 24 h in PC14 cells.

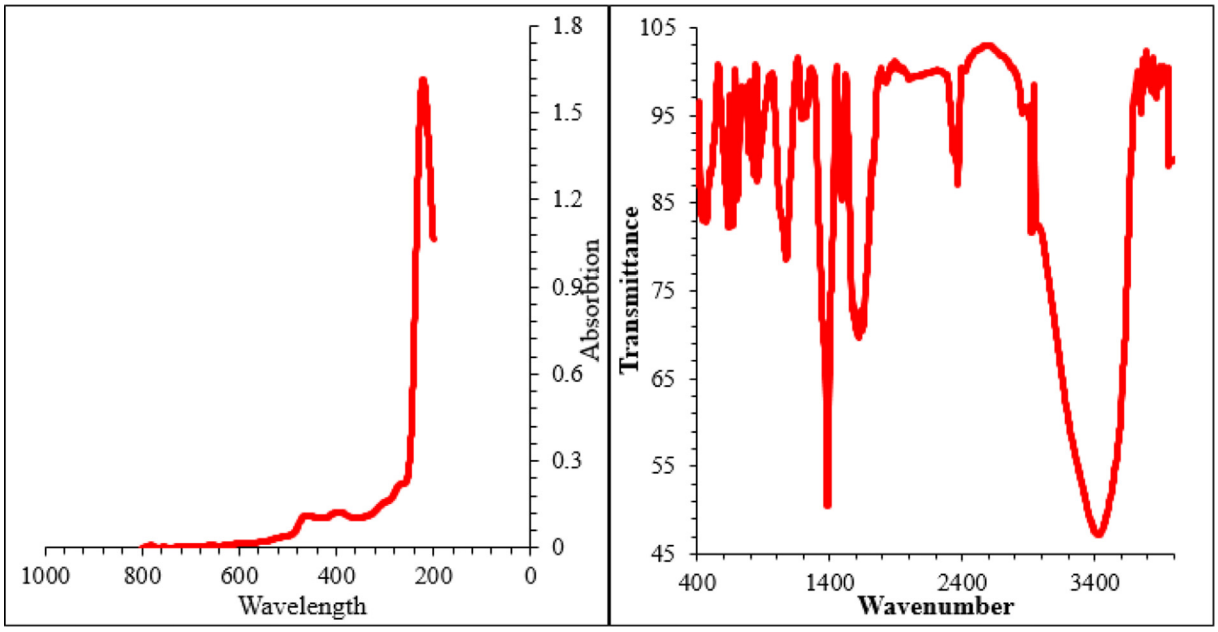

Fig. 1. Characterization of synthesized Zn-Ni NPs by UV–Vis and FT-IR.

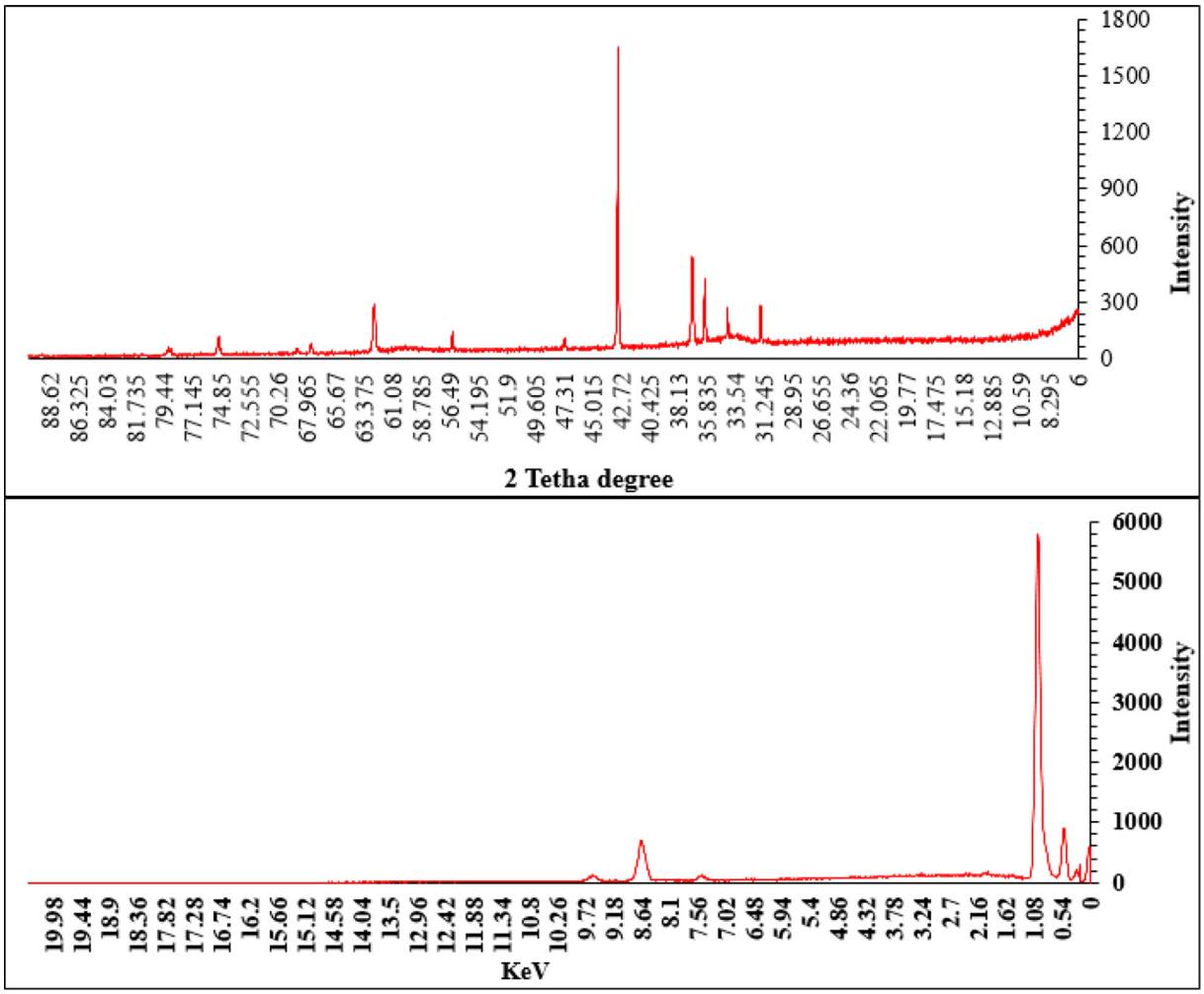

Fig. 2. Characterization of synthesized Zn-Ni NPs by XRD and EDX.

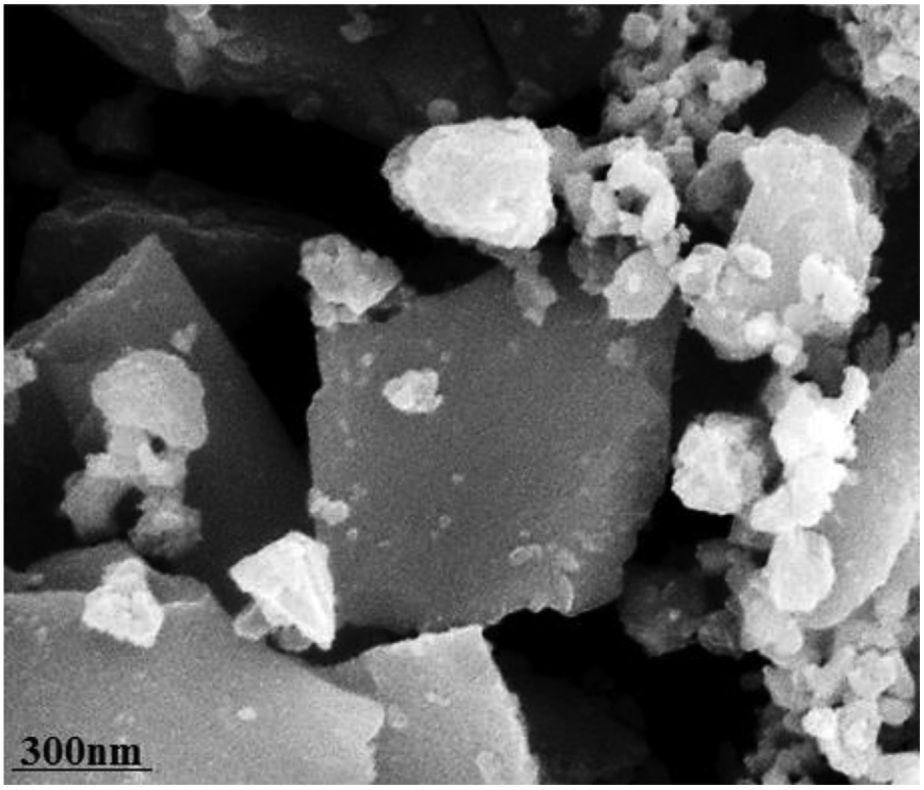

Fig. 3. Characterization of synthesized Zn-Ni NPs by FE-SEM.

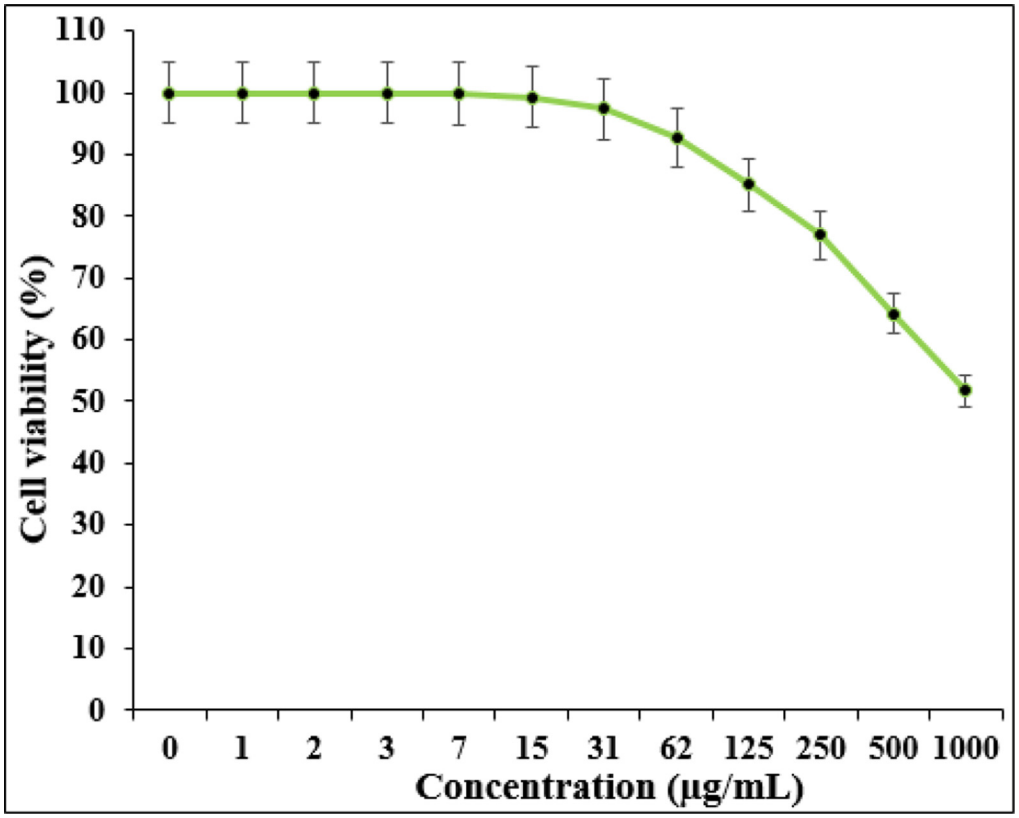

Fig. 4. Effect of Zn-Ni NPs on the viability of HUVEC cells.

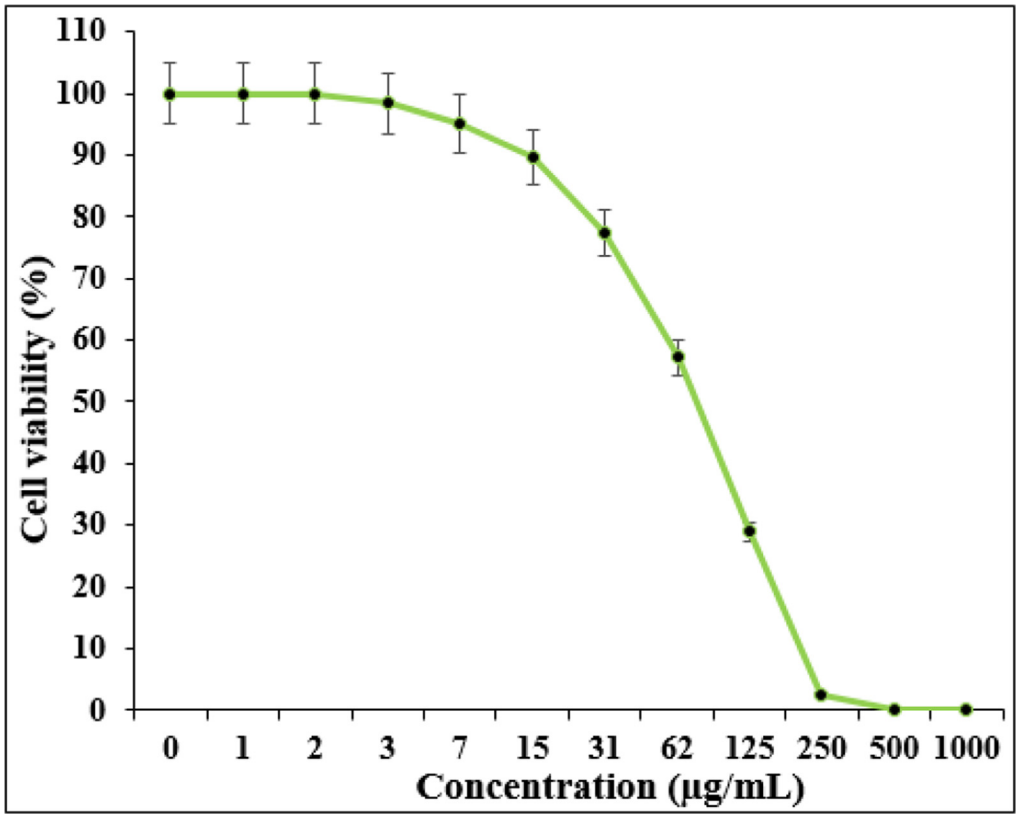

Fig. 5. Effect of Zn-Ni NPs on the viability of PC14 cells.

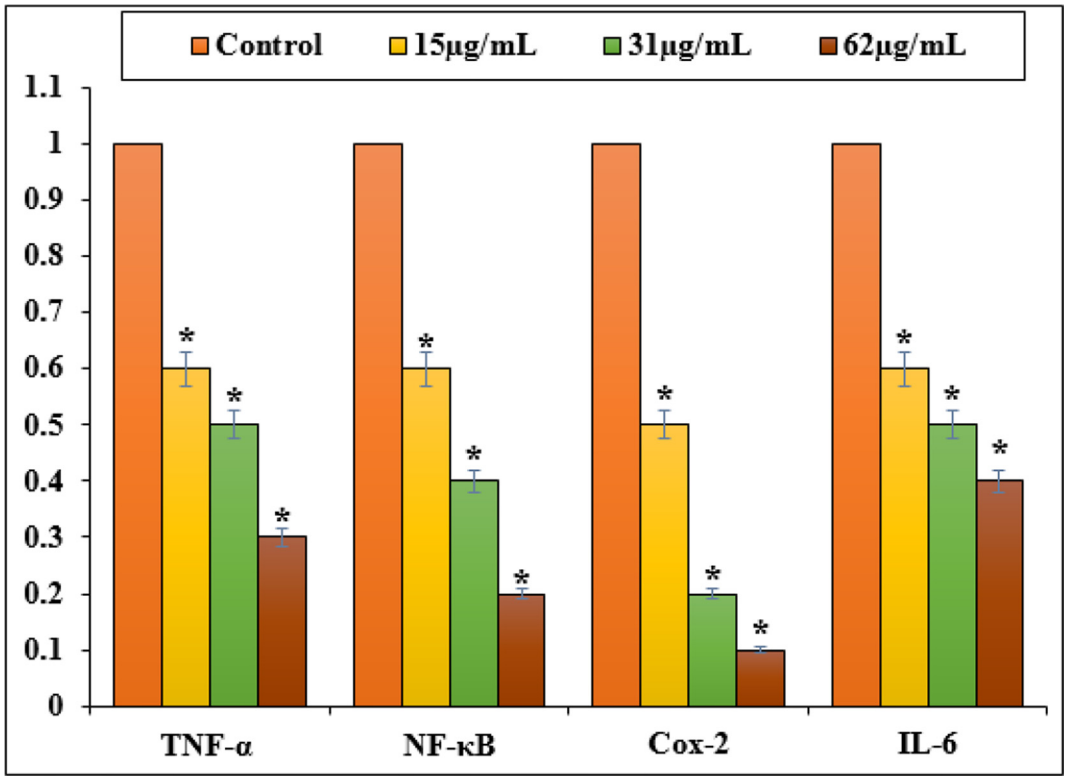

Fig. 6. Gene expression changes induced inflammatory response in PC14 cell line.

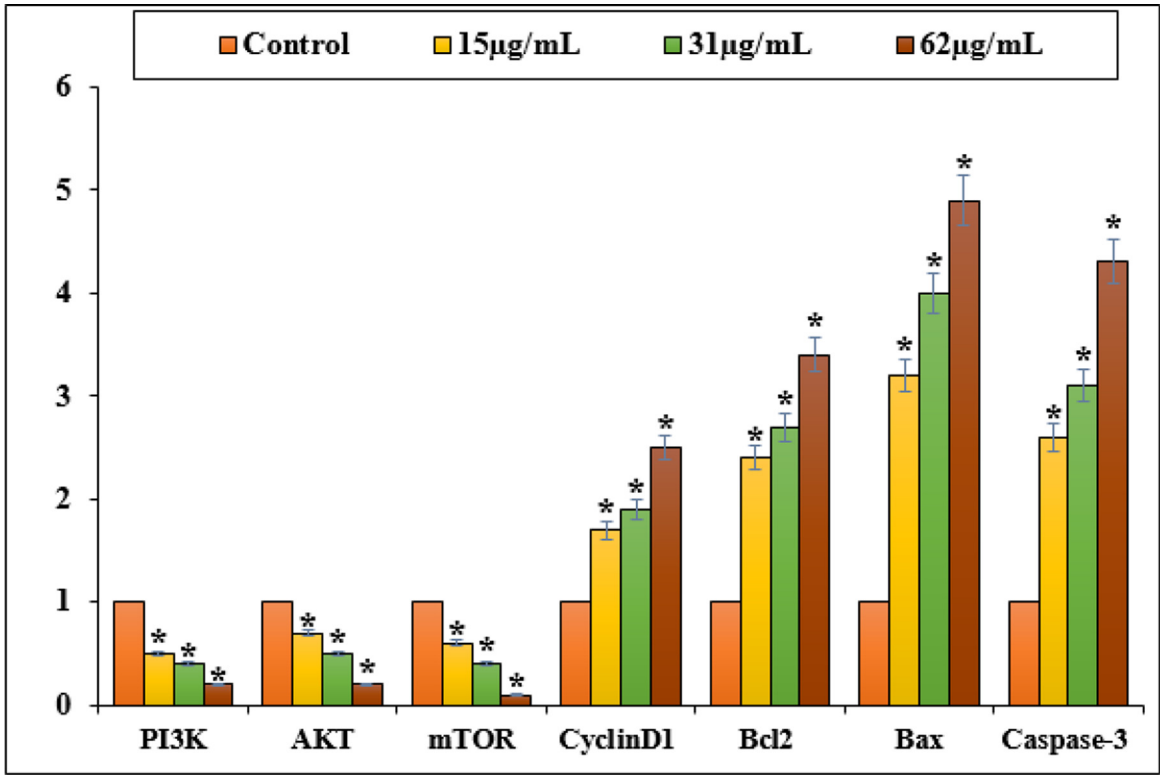

Fig. 7. Gene expression changes induced apoptosis in PC14 cell line.

To calculate the fold changes in gene expression levels within each cell type, we compared them to untreated cells from PC14. In this study, we observed an increase in pro-inflammatory gene expression after treating NOZ cells for 24 h with 15, 31, and 62 µg of Zn-Ni NPs.

As shown in Fig. 7, Zn-Ni NPs induced apoptosis in NOZ cells by down-regulating anti-apoptotic genes such as PI3K, AKT, mTOR, and CyclinD1 and upregulating pro-apoptotic gene Bcl2 and caspase-3. 15, 31, and 62 µg of Zn-Ni NPs decreased PI3K, AKT, mTOR, and CyclinD1 expression as well as bcl2 in a dose-dependently. NOZ cells, however, appear to undergo apoptosis by the caspase-dependent mitochondrial-mediated intrinsic pathway, as indicated by increases in Bax and caspase-3 expression.

4. Conclusion

In conclusion, we have herein established a green and biogenic procedure for the synthesis of Zn-Ni NPs by using *Curcuma longa* leaf extract. Morphological features of the material were demonstrated through a number of advanced analytic techniques. The Zn-Ni NPs were assessed in anticancer and cytotoxicity effects against lung cancer cells i.e. PC14. The viability of cancer cells decreased in the Zn-Ni NPs presence. PC14 cells phosphorylated mTOR, cyclin D1, Akt, and PI3K in response to Zn-Ni NPs. The Zn-Ni NPs also inhibited the phosphorylation of mTOR and Akt, reducing tumor volume and weight. Accordingly, Zn-Ni NPs might be promising candidate for lung cancer treatment.

Declaration of Competing Interest

The authors declare that they have no known competing financial interests or personal relationships that could have appeared to influence the work reported in this paper.

Acknowledgments

We would like to convey thanks to all colleagues who supported us during this research. Special thanks to the staff of Yantaishan Hospital and Yantai Yuhuangding Hospital for their support.

References

Borm, P.J., Robbins, D., Haubold, S., 2006. The potential risks of nanomaterials: a review carried out for ECETOC. Part. Fibre Toxicol. 3 (1), 11.

Bray, F., Ferlay, J., Soerjomataram, I., Siegel, R.L., Torre, L.A., Jemal, A., 2018. Global cancer statistics 2018: GLOBOCAN estimates of incidence and mortality worldwide for 36 cancers in 185 countries. CA Cancer J. Clin. 68 (6), 394–424.

Budarin, V.L., Clark, J.H., Luque, R., Macquarrie, D.J., White, R.J., 2008. Green Chem. 10, 382–387.

Cancer of the Lung and Bronchus-Cancer Stat Facts. [(accessed on 9 November 2022)]; Available online: https://seer.cancer.gov/statfacts/html/lungb.html.

Cancer Today. [(accessed on 21 December 2022)]. Available online: http://gco.iarc.fr/today/home.

Cheng, Z., Li, M., Dey, R., Chen, Y., 2021. Nanomaterials for cancer therapy: Current progress and perspectives. J. Hematol. Oncol. 14, 85.

Dehnoee, A., Kalbasi, R.J., Zangeneh, M.M., Delnavazi, M.R., Zangeneh, A., 2023. One-step synthesis of silver nanostructures using Heracleum persicum fruit extract, their cytotoxic activity, anti-cancer and anti-oxidant activities. Micro & Nano Lett. 18 (1), e12153.

Elkhenany, H., Abd Elkodous, M., Ghoneim, N.I., Ahmed, T.A., Ahmed, S.M., Mohamed, I.K., El-Badri, N., 2020. Int. J. Biol. Macromol. 143, 763–774.

Gholami, L., Ivari, J.R., Nasab, N.K., Oskuee, R.K., Sathyapalan, T., Sahebkar, A., 2023. Recent advances in lung cancer therapy based on nanomaterials: A review. Curr. Med. Chem. 30, 335–355.

Gospodarowicz, M., Brierley, J., O'Sullivan, B., 2015. Principles of cancer staging for clinical obstetrics and gynecology. Best Pract. Res. Clin. Obstet. Gynaecol. 29, 767–775.

(a) Han Y, Gao Y, Cao X, Zangeneh MM, Liu S, Li J. Int. J. Biol. Macromol. 2020;164:2974-2986. (b) Han S, Ahmeda A, Jalalvand AR, Lu W, Zangeneh MM, Zangeneh A. Appl. Organomet. Chem. 2022; 36(12): e5491. (c) Abbasi N, Ghaneialvar H, Moradi R, Zangeneh MM, Zangeneh A. Arab J Chem. 2021; 14(7): 103246. (d) Ma D, Gong D, Han T, Javadi M, Mohebi H, Karimian M, Abbasi N, Ghaneialvar H, Zangeneh MM, Zangeneh A, Shahriari M, Zhang F, Sun J, Liu Y. Int. J. Biol. Macromol. 2021;165:767–775.

Itani, R., Al Faraj, S.A., 2019. siRNA conjugated nanoparticles-A next generation strategy to treat lung cancer. Int. J. Mol. Sci. 20 (23), 6088.
Khalid, K., Tan, X., Mohd Zaid, H.F., Tao, Y., Lye, C.C., Chu, D.-T., Lam, M.K., Ho, Y.-C., Lim, J.W., Chin, W.L., 2020. Advanced in developmental organic and inorganic nanomaterial: A review. Bioengineered 11, 328–355.
Lademann, J., Richter, H., Teichmann, A., Otberg, N., Blume-Peytavi, U., Luengo, J., Weiss, B., Schaefer, U.F., Lehr, C.M., Wepf, R., Sterry, W., 2007. Nanoparticles–an efficient carrier for drug delivery into the hair follicles. Eur. J. Pharm. Biopharm. 66 (2), 159–164.
Li, G.; Liu, D.; Zuo, Y.Y. Nano-bio Interactions in the Lung. In Nanomedicine; Springer: Berlin/Heidelberg, Germany, 2022; pp. 1–31.
Liu, D., Chen, L., Jiang, S., 2014. Formulation and characterization of hydrophilic drug diclofenac sodium-loaded solid lipid nanoparticles based on phospholipid complexes technology. J. Liposome Res. 24 (1), 17–26.
Liu, Z.Y., Xu, G.L., Tao, H.H., Yang, Y.Q., Fan, Y.Z., 2017. Establishment and characterization of a novel highly aggressive gallbladder cancer cell line, TJ-GBC2. Cancer Cell Int. 17, 20.
Ma, L., Ahmeda, A., Wang, K., Jalalvand, A.R., Sadrjavadi, K., Nowrozi, M., Zangeneh, A., Zangeneh, M.M., Wang, X., 2022. Introducing a novel chemotherapeutic drug formulated by iron nanoparticles for the clinical trial studies. Appl. Organomet. Chem. 36 (12), e5498.
Mottaghitalab, F., Farokhi, M., Fatahi, Y., Atyabi, F., Dinarvand, R., 2019. New insights into designing hybrid nanoparticles for lung cancer: Diagnosis and treatment. J. Control. Release 295, 250–267.
Patra, J.K., Das, G., Fraceto, L.F., Campos, E.V.R., Rodriguez-Torres, M.D.P., Acosta-Torres, L.S., DiazTorres, L.A., Grillo, R., Swamy, M.K., Sharma, S., 2018. Nano based drug delivery systems: Recent developments and future prospects. J. Nanobiotechnol. 16, 71.
Shaabani, A., Rahmati, A., Badri, Z., 2008. Catal. Commun. 9, 13–16.
Siegel R.L., Miller K.D., Fuchs H.E., Jemal A. Cancer Statistics, 2022. CA: A Cancer J. Clin. 2022;72:7–33. doi: 10.3322/caac.21708.
Stapleton P.A. and Nurkiewicz T.R. 2014. Vascular distribution of nanomaterials. Wiley Interdisciplinary Reviews. *Nanomedicine and nanobiotechnology*. 6(4), pp. 338-348.
Trojer, M.A., Li, Y., Wallin, M., Holmberg, K., Nyden, M., 2013. Charged microcapsules for controlled release of hydrophobic actives Part II: surface modification by Lbl adsorption and lipid bilayer formation on properly anchored dispersant layers. J. Colloid Interface Sci. 409, 8–17.
Virlan, M.J.R., Miricescu, D., Radulescu, R., Sabliov, C.M., Totan, A., Calenic, B., Greabu, M., 2016. Organic nanomaterials and their applications in the treatment of oral diseases. Molecules 21, 207.
(a) Zangeneh MM, Zangeneh A. Appl. Organomet. Chem. 2020;34(3):5374. (b) Zangeneh A, Kalbasi RJ, Seydi N, Zangeneh MM, Mansouri S, Goorani S, Moradi R. Appl. Organomet. Chem. 2020;34(4):e5358. (c) Zangeneh A, Zangeneh MM. Appl. Organomet. Chem. 2020;34(2):e5378. (d) Zangeneh MM. Appl. Organomet. Chem. 2020;34(1):e5295.